A Novel method to trace flicker sources

M. Poormonfaredazimi*, H. Moghadam*, A. Doroudi*
*Electrical of Engineering of Department, Shahed University, Tehran, Iran
e-mail: mo.azimi@shahed.ac.ir, moghadam1.hadi@gmail.com, doroudi@shahed.ac.ir

دبیرخانه کنفرانس: خیابان فلسطین، شماره ۴۶۳، ساختمان ۵۵
انجمن مهندسین برق و الکترونیک ایران
www.epdc.ir ,www.laeee-iran.org, info@epdc.ir
تلفن: ۸۸۶۲۳۳۴۰و ۸۸۸۹۵۱۵۹ فاکس: ۸۸۶۲۳۳۴۱و ۸۸۹۰۴۱۵۸

Abstract- Voltage flicker is a common phenomenon of power quality problems which is referred to as voltage low frequency fluctuations modulated on carrier signal. Voltage flicker creates some variations in network voltage. In order to mitigate flicker, the flicker source should be identified. This paper proposes a novel method to determine the direction of flicker flow by using flicker power measurement. At first, low frequency fluctuations are separated from monitored signals by using coherent phase demodulation and wavelet transform. Then the flicker power is computed via voltage and current envelopes. The direction of flicker flow in network is obtained from the sign of the flicker power. The proposed algorithm has been validated by simulations.

Keywords: Flicker, Flicker Assessment, Flicker Power Flow, IEC 61000-4-15, Power Quality

I- Introduction

Consumers generally expect high power supply quality from utilities. But for various reasons they encounter with unexpected distortions and fluctuations in their power supply which may cause equipment disconnection and possibly devices damage. In the early years of invention of electricity and use of electrical energy, people often dealt with the event of light flicker that was uncomfortable to human eyes. With the increasing requirement of modern customers for power quality, in addition to customers' complains, voltage fluctuations or flicker problems have received more attention by utilities [1].

One of the most harsh power quality events is voltage flicker. Voltage flicker is referred to the periodical or stochastic changes of voltage waveform which originates from the fast heavy loads such as motors, arc furnaces, rolling mills, welding machines and etc [2],[3]. The wind farms will also produce voltage fluctuations [4], [5].

Generally, while voltage fluctuations exceed certain magnitude for certain repetition frequencies, given in standard IEC 61 000-4-15 [6], it is observed by human eyes as a disturbing unsteadiness of the light intensity. As it is mentioned in the standard, voltage flicker has frequencies less than the network frequency and it is visible and recognizable in the frequency range of 0.5 to 35 Hz (flicker frequency window). The magnitude of fluctuations is within ±10%. The fluctuations have a direct impact on lights flicker. Moreover, the phenomenon causes some noises in TV sets and incorrect operation of clinical equipments such as ICU and CCU systems (These equipments depending on different amplitudes of supply voltage, present different reports of the patients).

So far various methods for flicker measurement are proposed. The most comprehensive method is presented in standard IEC 61 000-4-15. In the method of the standard, values of short term (P_{st}) and long term (P_{lt}) flicker levels are measured. Unfortunately, both of the levels provide the flicker amount at the monitoring point without any information regarding the flicker direction in power network. Moreover these quantities are not able to identify the dominating flicker sources. Identification of flicker source is of great interest for both utilities and customers. In fact, mitigation of flicker requires identification of flicker source.

A few works has been presented within this topic which is not based on standard IEC 61000-4-15 [7-13]. The method proposed in [14,15] developed an analytical approach to determine the direction of flicker source with respect to monitoring point in the same way as defined in the IEC 61000-4-15. Both of the papers are based on a new quantity called "flicker power" which is production integration of envelopes of the voltage and current amplitude modulating signals. The envelopes of the modulating signals should be obtained via demodulating process and by using some suitable filters. Sign of the flicker power applies to determine the direction to a flicker source. A positive sign indicates an upstream flicker source while the negative sign shows downstream ones with respect to a measuring point. One disadvantage of the both method presented in [14,15] is that they generate additional low frequency components in flicker frequency window which make them impossible to superpose flicker

power correctly. In addition, the methods sometimes do not provide the correct answer about the flicker direction and identification the dominant flicker source.

In this paper a novel algorithm based on coherent detector and wavelet transform is proposed in order to improve the method presented in [14,15]. The new algorithm can be used for detecting the dominant flicker source from a multiflicker source network which contains any frequencies within flicker frequency range.

II. Network Contains Flicker Sources

Consider a simple network containing multiple flicker sources (loads $Z_{F.S.1}$, $Z_{F.S.2}$) as shown in Fig. 1:

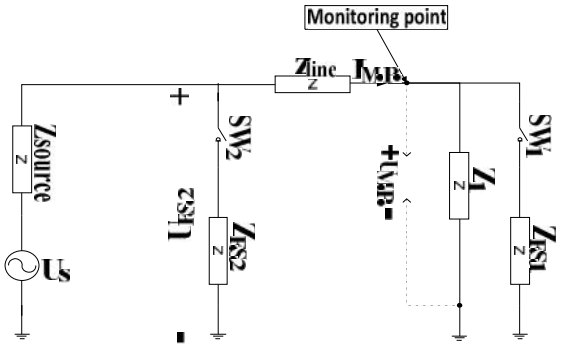

Fig. 1. Circuit model for multiple flicker sources

The circuit consists of a constant voltage source, a source impedance Z_{source} , a transmission line impedance Z_{line} and Z_1 , $Z_{F.S.1}$ and $Z_{F.S.2}$ that are linear impedances. When the switches SW1 and SW2 operate with frequency f_m (which is within the frequency flicker range), $Z_{F.S.1}$ and $Z_{F.S.2}$ can be considered as flicker sources.

When SW1 and SW2 are open (off), U_S can be obtained as:

$$U_S = (Z_{source} + Z_{line}) I_{M.P.} + U_{M.P.} \qquad (1)$$

Now assume two cases in the above circuit:

Case 1) SW1: ON and SW2: OFF

While SW2 is closed, we have:

$$\begin{aligned} U_S &= (Z_{source} + Z_{line})(I_{M.P.} + \Delta I) + U'_{M.P.} \\ &= (Z_{source} + Z_{line}) I_{M.P.} + (Z_{source} + Z_{line}) \Delta I + U'_{M.P.} \\ &= (Z_{source} + Z_{line}) I_{M.P.} + \Delta U + U'_{M.P.} \end{aligned} \qquad (2)$$

where ΔI is the current through $Z_{F.S.1}$. Variation of voltage due to SW1 switch operation is:

$$U'_{M.P.} - U_{M.P.} = -\Delta U \qquad (3)$$

and corresponding changes in current should be:

$$I_{M.P.} \rightarrow I_{M.P.} + \Delta I \qquad (4)$$

Therefore, when SW1 is closed the voltage across Z_1 decreases, but its' through current increases. In other words, an increase in current will lead to a decrease in the voltage. These variations are shown in Fig.2. The figure depicts that the voltage and current envelopes are in opposite phase.

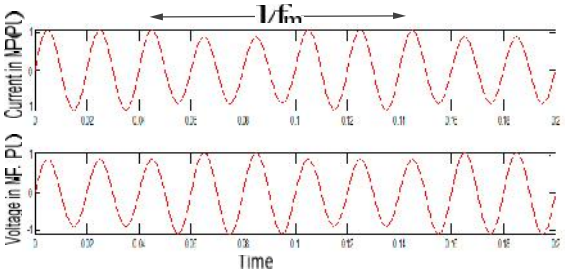

Fig. 2: Variations of current and voltage envelopes due to operation of downstream flicker source

Case 2) SW1: OFF and SW2: ON

In this case, $U_{F.S.2}$ is obtained as:

$$U_{FS2}=\frac{U_S}{Z_{source}+Z_{FS2}\|(Z_{line}+Z_1)}\times Z_{FS2}\|(Z_{line}+Z_1)$$
$$=\frac{U_S(Z_{line}+Z_1)Z_{FS2}}{Z_{source}(Z_{line}+Z_1+Z_{FS2})+(Z_{line}+Z_1)Z_{FS2}}$$
$$=\frac{U_S.(Z_{line}+Z_1)}{Z_{source}(1+\frac{Z_{line}+Z_1}{Z_{FS2}})+(Z_{line}+Z_1)} \qquad (5)$$

current $I_{M.P.}$ is thus calculated as:

$$I_{M.P.}=\frac{U_{F.S.2}}{(Z_{line}+Z_1)}=\frac{U_S}{Z_{source}.(\frac{Z_{line}+Z_1}{Z_{F.S.2}}+1)+(Z_{line}+Z_1)} \qquad (6)$$

and the voltage $U_{M.P.}$ is equal to:

$$U_{M.P.}=I_{M.P.}.Z_1=\frac{U_S}{Z_{source}.(\frac{Z_{line}+Z_1}{Z_{F.S.2}}+1)+(Z_{line}+Z_1)}.Z_1 \qquad (7)$$

The voltage and current envelopes variations are shown in Fig. 3.

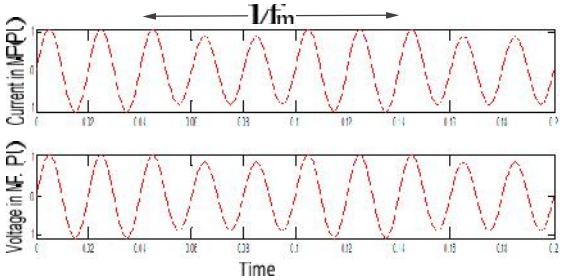

Fig. 3: Variation of current and voltage envelopes due to operation of upstream flicker source

As it is shown from the figure, the changes in current will follow the voltage. It means that the envelopes in the voltage and current are in phase.

To sum up, two observations can be obtained from the above cases:

1) The flicker source causes variation in the current and voltage envelopes at the monitoring point. In other word, because of flicker source, the waveforms in voltage and current are amplitude modulated due to the variation in the voltage and current amplitudes.
2) Envelopes of the amplitude modulated voltage and current signals are in-phase for flicker source that is placed upstream, and are 180° out-of-phase for flicker source that is located downstream with respect to the monitoring point.

III. Flicker Power Analysis

If the voltage and current signals being amplitude modulated (AM), they can be expressed as:

$$u(t) = (U_C + m_u(t))Cos(\omega_C t + \alpha)$$
$$i(t) = (I_C + m_i(t))Cos(\omega_C t + \beta) \qquad (8)$$

where $U_C Cos(\omega_C t + \alpha)$ and $I_C Cos(\omega_C t + \beta)$ represents fundamental carrier signals of voltage and current, respectively. The envelopes or low frequency fluctuations are represented by $m_u(t)$ and $m_i(t)$. Then, the instantaneous flicker power $FP(t)$ is defined as:

$$FP(t) = m_u'(t).m_i'(t) \qquad (9)$$

where $m_u'(t)$ and $m_i'(t)$ are obtained from $m_u(t)$ and $m_i(t)$ using the sensitivity filter presented in IEC 61000-4-15.

The flicker power FP is defined as:

$$FP = \frac{1}{T}\int_{t}^{t+T} m_u'(\tau).m_i'(\tau)d\tau \qquad (10)$$

where T is the time of integration [15]. A positive sign of FP indicates an upstream flicker source while the negative sign indicates downstream flicker source with respect to a monitoring point.

The proposed block diagram for calculating of flicker power is shown in Fig. 4.

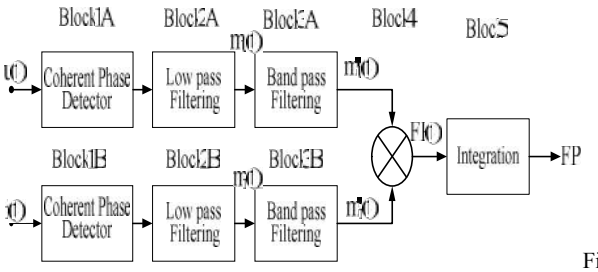

Fig. 4. Proposed block diagram for flicker power calculation

Blocks 1 to 3 are identical for both current and voltage signals. The modulating signals are extracted by a demodulation method performed in block 1 and 2. The band-pass filter in blocks 3A/3B is the flicker sensitivity filter with a transfer function defined in IEC 61000-4-15. The output of these blocks are a band-pass filtered version of $m_u(t)$ and $m_i(t)$ named $m_u'(t)$ and $m_i'(t)$. $m_u'(t)$ and $m_i'(t)$ is finally

multiplied and integrated (block 4 and 5) resulting in flicker power FP . Details of the blocks will be described in the following.

A. Demodulation Process

To separate $m_u(t)$ and $m_i(t)$ from the carrier signals, $u(t)$ and $i(t)$ should be demodulated. In [14], the "square demodulation" was proposed for this goal. The method operates as a nonlinear function and it generates additional low frequency components within the flicker frequency window which makes it to impossible apply superposition theorem to flicker power (Fig. 5). In [15] envelope detector is proposed instead of square demodulation method. In this case, an additional frequency component is produced at the frequency range $\omega_c - \omega_m$ where ω_m is the flicker frequency (Fig. 6). Assume that the network frequency is 50Hz. It is seen that an additional frequency component will locate within the flicker frequency window (0-35Hz) while the flicker source frequency being above 15Hz. The method is not thus able to calculate the correct flicker power at the all of the flicker source frequencies.

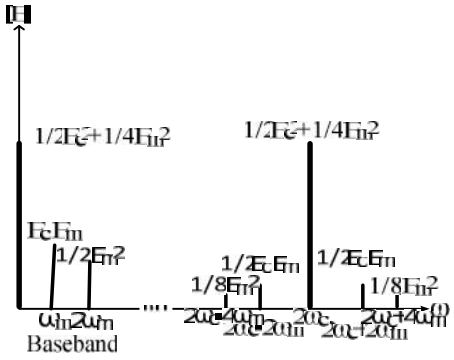

Fig.5: Frequency spectrum of square detector output

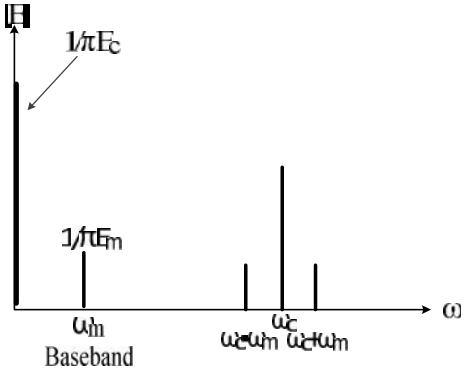

Fig.6: Frequency spectrum of envelope detector output

In this paper, coherent detector is proposed in order to improve the demodulation process (Fig. 7). The outputs of this detector will only contain a DC component and a low-frequency fluctuation within the flicker frequency window (Fig. 8).

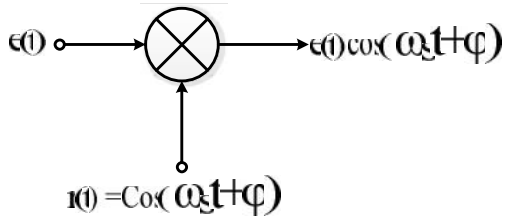

Fig. 7. Coherent detector principle

In the coherent demodulation, first the amplitude modulated signal $e(t)$ is multiplied by a sinusoidal signal $r(t) = Cos(\omega_s t + \varphi)$ which has the same frequency and phase angle as the network (carrier) signal. Let's the amplitude modulated signal $e(t)$ is expressed as follows:

$$e(t) = (E_C + m(t))Cos(\omega_C t + \alpha) \qquad (11)$$

By multiplying $e(t)$ to the sinusoidal signal with frequency ω_s and phase angle φ, we have *:*

$$e(t)r(t) = (E_C + m(t))Cos(\omega_C t + \alpha).Cos(\omega_s t + \varphi) = [E_C + m(t)]$$
$$\times 0.5[Cos((\omega_C - \omega_s)t + (\alpha - \varphi)) + Cos((\omega_C + \omega_s)t + (\alpha + \varphi)] \qquad (12)$$

If $\omega_s = \omega_C$, $\varphi = \alpha$, $e(t) \times r(t)$ is thus given as below*:*

$$e(t).r(t) = (E_C + m(t))Cos^2(\omega_C t + \alpha) \qquad (13)$$

For $m(t) = E_m Cos(\omega_m t)$, the equation (13) results in:

$$e(t).r(t) = (E_C + E_m Cos(\omega_m t)).1/2(1 + Cos(2\omega_C t + 2\alpha)) \qquad (14)$$

The frequency spectrum of the coherent detector output according to equation (14) is shown in Fig. 8.

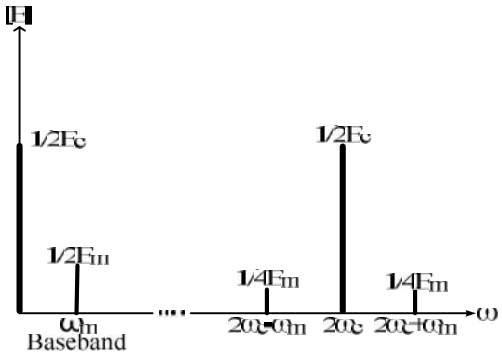

Fig.8: Frequency spectrum of coherent detector output

Fig. 8 shows that coherent detector is more appropriate comparing with square and envelope detectors. It is due to its frequency response which only contains a DC component and a low-frequency fluctuation in the baseband. The other components do not locate within the flicker frequency window for any feasible flicker source frequency. Then the superposition theorem can be applied to flicker power and this parameter will be a conservative quantity. The only drawback of this type of detector is that it requires the detailed and exact knowledge of the frequency and phase angle of the network signal. In this paper, in order to obtain the frequency and phase angle of the network signal the wavelet transform will be used.

B. Principle of wavelet transform

Wavelet transform has recently become well known as a useful tool in power system analysis which does not have the FFT problems. If x(t) is a time-varying signal, the continuous wavelet transform is defined as below:

$$CWT(\tau,a)=|a|^{-\frac{1}{2}}\int_{-\infty}^{+\infty}X(t)\varphi^{*}(\frac{t-\tau}{a})dt \qquad (15)$$

where τ and a are transport and scale parameters, respectively. $\varphi(t)$ is the wavelet function and $\varphi^{*}(t)$ is the complex conjugate of $\varphi(t)$. Wavelet function should satisfy the requirement of equation (16):

$$\int_{-\infty}^{+\infty}\varphi(t)dt=0 \qquad (16)$$

In order to analysis various phenomena of the power network, different wavelet functions can be used such as Symlet, Morlet and Daubechies. Feasibility of each basis function depends on the application requirements. In [16], the Morlet wavelet was selected as the wavelet basis function for the voltage flicker study. In this paper, the modulated Gaussian wavelet was selected for frequency identification of carrier signal. The Gaussian wavelet formulation is exponential function-based and is symmetrical about zero. The function also satisfies the requirement of equation (16). By utilizing the Gaussian wavelet transform, it is of high flexibility in monitoring any frequency of interest in a waveform [17]. The formulation of this function is given as bellow:

$$\varphi(t)=\exp(j2\pi F_0 t-0.5t^2) \qquad (17)$$

where F_0 is the signal frequency. In this study, we select $F_0=25\pi$.

In the flicker study, the modulated voltage can be expressed as follows:

$$U(t)=\sqrt{2}\left[v+\sum v_m Sin(2\pi f_m t+\alpha_m)\right]Sin(2\pi ft+\alpha)$$
$$=\sqrt{2}vSin(2\pi ft+\alpha)+\sum\frac{v_m}{\sqrt{2}}Cos[2\pi(f-f_m)t+\alpha_m^{-}]-$$
$$\sum\frac{v_m}{2}Cos[2\pi(f+f_m)t+\alpha_m^{+}] \qquad (18)$$

Where v is the reference root-mean-square (rms) value of the network voltage signal without flicker, f is the network frequency, f_m is the flicker *m*th component (flicker demodulation) frequency, and v_m is the flicker *n*th component amplitude (flicker modulation depth) at f_m. α and α_m are basis voltage and flicker *m*th component phase angle, respectively.

The discrete version of wavelet transform (equation 15) is expressed as follows:

$$CWT(a,T_s)=T_s.\sum_{n=1}^{N_a}v(nT_s).\varphi^{*}\left[\frac{nT_s}{a}-\frac{N_{dw}.T_s}{2}\right] \qquad (19)$$

Where $v(nT_s)$ is the sampled signal of $v(t)$, $\phi(nT_s)$ is the sampled version of $\phi(t)$ and N_a is equal to $a\times N_{dw}$. If a signal is sampled at the interval of T_{ds} for the duration of T_s, the number of samples will be $N_{ds}=\frac{T_{ds}}{T_s}$ where sampling

frequency is $f_s = \frac{1}{T_s}$. Now, if the wavelet function is sampled with the same sampling interval T_s, the duration will be equal to T_{dw} and $N_{dw} = \frac{T_{dw}}{T_s}$ where N_{dw} is the total number of samples. In this study, we assumed T_s=0.01 and $T_{dw} = T_{ds} = 2\pi$.

Firstly, the values of a_k are computed by equation (20) for any values of k, where k is an integer whose maximum value is $(f_h - f_l)/f_{ru}$. f_h and f_l are the maximum and minimum of network frequency and f_{ru} is the frequency resolution. Duo to regular network frequency changes, f_h=50.5 Hz, f_l =49.5 Hz and f_{ru}=0.01 have been assumed (k=1 to 100).

$$a_k = \frac{F_0}{f_l + kf_{ru}} \qquad (20)$$

By obtaining a set of different values of a_k, CWT can be calculated from equation (20).

Secondly, A_k is computed as bellow:

$$A_k = \frac{(a_k)^{\frac{1}{2}} |CWT(a_k)|}{T_{dw}} \qquad (21)$$

After all A_k are computed, for the maximum A_k, its corresponding frequency f_s is the network frequency. Now the CWT is computed again for a virtual signal with system frequency and zero phase angle. Then the computed virtual signal CWT compares with the real network signal CWT and the voltage amplitude and phase angle of the network signal are obtained.

C. Filter chain

The Low-Pass filter provided in block 2 eliminates all of the additional frequencies except flicker frequencies and DC component. The band-Pass filter provided in block 3 is identical to digital band-pass filter defined in IEC 61000-4-15. The standard applies the human sensitivity curve to the flicker signal. The transfer function of the IEC standard filter is as bellow:

$$F(s) = \frac{\gamma\omega_1 s}{s^2 + 2\lambda s + \omega_1^2} \times \frac{1 + s/\omega_2}{(1 + \frac{s}{\omega_3})(1 + \frac{s}{\omega_4})} \qquad (22)$$

The parameters of the equation (22) for a light with rated values 60W/230V are shown in Table 1:

Table 1: Filter coefficients for the transfer function(equation22)

γ =1.74802	λ=2π.4.05981
ω_1=2π.9.15494	ω_3= 2π.1.22535
ω_2= 2π.2.27979	ω_4 =2π.21.9

The frequency response of the IEC filter is shown in Fig. 8. As it can be seen, it peaks at the frequency 8.8 Hz. The attenuation of the filter matches with the human eye sensitivity curve presented in the standard IEC 61000 -4-15.

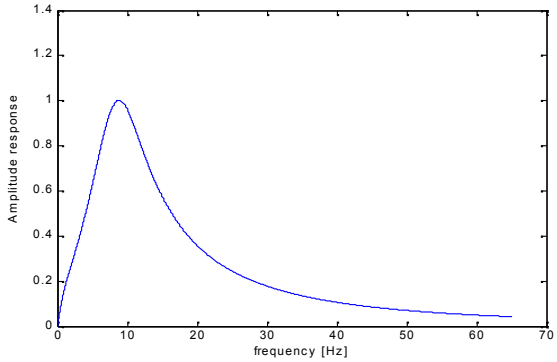

Fig. 8. Frequency response of band-pass filter

IV. Simulation Results

The simulations have been done using the MATLAB/SIMULINK software. The test network is shown in Fig. 9.The values of the network parameters are depicted in the figure. There are two flicker sources (arc furnace) in the network at bus 3 and 4 and three monitoring points $M.P_a$, $M.P_b$ and $M.P_c$ at bus 2 and two feeders connected to it.

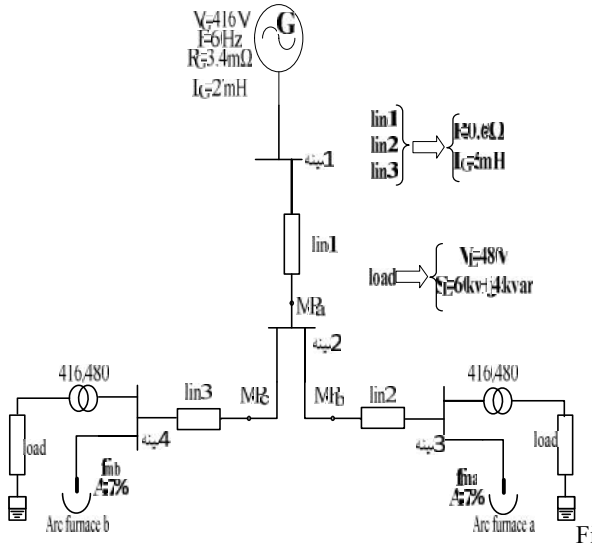

Fig. 9. Single-line diagram with two flicker sources

The characteristics of the flicker sources are shown in table 2 for three different cases. The simulations are done with the method presented in [14] (square demodulation), [15] (envelope demodulation) and with our proposed method (combined coherent detector and wavelet transform). The results have been shown in table 3 to 5.

Table 2 : Characteristic of Flicker sources in Fig. 9.

Table 3: Simulation results for method presented in [14]

Case	Flicker source A		Flicker source B	
	Depth %	Freq. Hz	Depth %	Freq. Hz
1	7%	9	7%	20
2	7%	9	7%	9
3	7%	9	7%	27

FP in M.P $_c$	FP in M.P $_b$	FP in M.P $_a$	Flicker frequency	
Square	Square	Square	f_{mb}	f_{ma}
$-3.325*10^4$	$-4.0946*10^5$	$-8.8539*10^5$	20	9
$-7.9534*10^5$	$-7.9534*10^5$	$-3.1814*10^6$	9	9
$-3.160*10^3$	$-4.106*10^5$	$-8.2749*10^5$	27	9

Table 4: Simulation results for method presented in [15]

FP in M.P $_c$	FP in M.P $_b$	FP in M.P $_a$	Flicker frequency	
Envelope	Envelope	Envelope	f_{mb}	f_{ma}
-0.12	-5.1793	-5.2993	20	9
-10.2215	-10.2215	-20.4435	9	9
0.2477	5.188	-4.946	27	9

Table 5: Simulation results for the proposed method

FP in M.P $_c$	FP in M.P $_b$	FP in M.P $_a$	Flicker frequency	
Coherent and wavelet	Coherent and wavelet	Coherent and wavelet	f_{mb}	f_{ma}
-0.456	-6.077	-6.53	20	9
-9.856	-9.856	-19.712	9	9

-0.04	-5.087	-5.127	27	9

As both of the flicker sources are downstream with respect to monitoring points, it is expected that the calculated flicker powers will be negative. Table 3 shows that the method in [14] predicts correctly the flicker direction for all of the cases, but the calculated FP cannot be superposed correctly. Then, the FP obtained from the square detector will not be a conservative quantity. Table 4 depicts that the method presented in [15] gives correct response for case 1 and 2. But for case 3, the method gives a positive FP which is an incorrect answer for this case. This is duo to the selected flicker frequency for flicker source B which generates additional low frequency component in the flicker frequency window which makes it presents an incorrect answer about the flicker direction. Table 5 shows that our proposed method gives correct FP for all three cases. Moreover, the results in table 5 confirm the superposition principle for the proposed method. Note that closer to the frequency 8.8Hz, bigger the calculated flicker power, e.g. for case 1, one can conclude that the flicker source A is the dominant flicker source.

V. Conclusion

In this paper, a method for identifying the flow direction of flicker and dominant flicker source has been presented. In this method, a coherent demodulation and a discrete wavelet transforms using Gaussian basis function has been applied for enhancement of flicker power measurement. By comparing with other methods, it was found that the proposed approach is more reliable in analyzing flicker power and gives correct response in any feasible frequency of flicker sources. This method causes the superposition principle can be applied to flicker power and this quantity became a conservative parameter. The proposed method is based on IEC 61000-4-15 and it is very efficient for identifying of flicker direction and dominant flicker source.

REFERENCES

[1] R.C Dugan, Electrical Power System Quality, 1996.

[2] S. Mendis, M. Bishop, and J. Witte. “Investigations of Voltage Flicker in Electric Arc Furnace Power Systems”. IEEE Industry Applications Magazine, Jan./ Feb. 1996.

[3] L. Toth and A. Hannan.”Calculation of Motor Flicker”. IEEE Conference paper 1993.

[4] Å. Larsson. “Flicker Emission of Wind Turbines during Continuous Operation”. IEEE Trans. On Energy Conversion. Vol. 17, pp. 114-118, Mar. 2002.

[5] J. Tande and K. Uhlen.”Wind Turbines in Weak Grids - Constraints and Solutions”.16th Int. Conf. on Electricity Distribution, CIRED 2001, June 2001.

[6] IEC Flicker meter—Functional and Design Specifications, IEC Std. 61000-4-15.

[7] K. Srinivasan. “rms fluctuations Attributable to a Single Customer” Power Quality Solutions, Sept. 1995.

[8]A. Dan. ” Identification of Flicker Sources”. Int. Conf. On Harmonics and Quality of Power. Athens, Greece, Oct. 1998.

[9] B. Hughes. “Source Identification for Voltage Sag and Flicker”. IEEE, Power Engineering Society Summer Meeting, 2000.

[10] M. Sakulin. “Field Experience with the Austrian UIE/IEC Flicker Analysis System”. Proc. of the 12th UIE Congress, Electrotech 92, pp.842-851, Montreal, Canada, 1992.

[11] M. Simoes and S. Deckmann.“Flicker propagation and attenuation”. Int. Conf. On Harmonics and Quality of Power. Oct. 1998.

[12] D. Zhang, W. Xu and A. Nassif. “Flicker Source Identification by Interharmonic Power Direction” .IEEE Canadian Conf. On Computer Engineering, May 2005.

[13] A. Hernandez, J. Mayordomo, R. Asensi and L. Beites. "A method based on interharmonics for flicker propagation applied to arc furnaces". IEEE Trans. On Power Delivery, Vol. 20, pp. 2334-2342, July 2005.

[14] P. G. V. Axelberg and M. H. J. Bollen, "An algorithm for determining the direction to a flicker source," IEEE Trans. on PWRD., Vol. 21, No.2, pp. 755–760, Apr. 2006.

[15] Peter G. V. Axelberg, "Math H. J. Bollen, Trace of Flicker Sources by Using the Quantity of Flicker Power" IEEE Trans. On PWRD, VOL. 23, No. 1, JANUARY 2008.

[16] Shyh-Jier Huang, "Enhancement of Digital Equivalent voltage Flicker Measurement via Continuous Wavelet Transform," IEEE Trans. Power Delivery, Vol. 19, No. 2, April. 2004.

[17] G. Strang and T. Nguyen,"Wavelets and Filter Banks", Cambridge, MA: Wellesley-Cambridge, 1997.